

Empirical-potential study of the dissociative chemisorption of Si_2H_6 on the $\text{Si}(001)2\times 1$ surface

Jian-Zhong Que,* M. W. Radny, and P. V. Smith

Physics Department, University of Newcastle, Callaghan, New South Wales, Australia 2308

(Received 28 September 1998; revised manuscript received 11 March 1999)

Molecular dynamics simulations and potential energy calculations have been performed to investigate the dissociative chemisorption of disilane (Si_2H_6) on the $\text{Si}(001)2\times 1$ surface. These calculations have been carried out using the extended Brenner (XB) empirical potential. The minimum energy atomic configurations for SiH_3 , SiH_2 , and H-Si-Si-H (Si_2H_2) species chemisorbed on the $\text{Si}(001)2\times 1$ surface have been determined. The chemisorption of SiH_3 radicals has been observed to occur predominantly at the dangling bond sites of the $\text{Si}(001)$ surface. The most stable SiH_2 configurations are found to be the on-dimer and intrarow structures. Seven different Si_2H_2 chemisorption structures have been investigated and the on-dimer-*B* structure found to be the most energetically favorable. These theoretically predicted structures are discussed in the light of recent experimental studies. Comparison of the results of these XB potential energy calculations with all-electron *ab initio* cluster calculations has also been made for a number of these different chemisorption structures. [S0163-1829(99)13135-7]

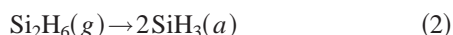
I. INTRODUCTION

The epitaxial growth of silicon atoms on the $\text{Si}(001)$ surface from hydride precursors such as disilane (Si_2H_6) is important in the production of silicon based semiconductor electronic devices. Disilane has been found to be a promising candidate for use in a variety of thin-film technologies such as low-temperature chemical vapor deposition (CVD),¹⁻³ UV-laser-induced CVD (LCVD),^{4,5} atomic-layer epitaxy,⁶⁻⁸ and gas-source molecular-beam epitaxy (GS-MBE).^{9,10} Disilane has also exhibited significantly greater reactivities on Si than either SiH_4 or SiH_2Cl_2 ,^{1,2,11,12} and a lower activation energy for gas-phase decomposition.^{13,14} A detailed knowledge of the fundamental processes underlying the decomposition of disilane on silicon surfaces is thus clearly important in understanding and optimizing the growth of epitaxial silicon on silicon substrates.

The dissociative chemisorption of disilane on silicon surfaces has been widely studied.^{1-11,15-28} Gates and Chiang¹⁵ have proposed two possible reaction processes for the initial dissociation of disilane on the $\text{Si}(001)2\times 1$ surface, namely



and



where (*a*) denotes adsorption on the surface, and (*g*) denotes the gas phase. Of these two reaction processes, the dissociation of disilane into SiH_3 fragments has been most widely accepted.^{6,19,21,23-25}

Suda *et al.*¹⁹ have proposed a two-stage adsorption process for disilane on the $\text{Si}(001)2\times 1$ surface. In this two-stage process, the disilane initially dissociates into silyl (SiH_3) radicals via scission of the Si-Si bond. These SiH_3 radicals adsorb onto adjacent dangling bonds of the clean surface. The adsorbed SiH_3 then decompose to silylene (SiH_2) and H, which leads to the formation of a 2×1 monohydride surface. Once all of the dangling-bond sites are satu-

rated, further (Si_2H_6) exposure converts the monohydride 2×1 phase into the 1×1 dihydride phase.

In recent scanning tunneling microscopy (STM) experiments of the interaction of disilane with the $\text{Si}(001)2\times 1$ surface, Bronikowski *et al.*²⁴ have observed roughly equal numbers of chemisorbed H atoms and SiH_2 complexes. They argue that this is strong evidence for the dissociation of disilane into two SiH_3 fragments, which subsequently dissociate into SiH_2 and H. They also proposed several possible chemisorption sites for SiH_2 radicals on the $\text{Si}(001)2\times 1$ surface and identified the occurrence of the so-called intrarow bonding configuration in which the SiH_2 radical is bridge bonded across the ends of two adjacent dimers of the same row. In a subsequent publication,²⁵ this group presented STM images showing SiH_3 fragments chemisorbed onto the dimer dangling bonds, and randomly distributed over the surface. At low coverage, these SiH_3 fragments were found to be unstable and to dissociate into SiH_2 and H on a time scale of tens of minutes. They also reported the observation of H-Si-Si-H fragments on the $\text{Si}(001)2\times 1$ surface, and postulated a mechanism whereby two intrarow SiH_2 groups bond together to form a hydrogenated dimer oriented parallel to the substrate dimers.

Bowler and Goringe²⁶ have calculated the minimum energy configurations of four possible adsorption sites for SiH_2 molecules on the $\text{Si}(001)2\times 1$ surface using the local-density approximation (LDA) density-functional method. Their results predict the intrarow site to be the most stable SiH_2 adsorption site, although the adsorption energy for the on-dimer site was found to differ by less than 0.01 eV. Owen *et al.*²⁷ investigated the growth of silicon from disilane using scanning tunneling microscopy. They observed a novel square structure consisting of four silicon atoms on the $\text{Si}(001)$ surface after exposure to small amounts of disilane at temperatures between 400 and 600 K. Using tight-binding and density-functional theory (DFT) calculations they found this square structure to be energetically stable with respect to isolated ad-dimers.

Based on their observations during synchrotron radiation stimulated disilane gas-source molecular-beam epitaxy (SR-GSMBE) on the Si(100) surface at temperatures ≤ 400 °C, Yoshigoe *et al.*²⁸ have reported that the number of different SiH_x species on the surface depends on the substrate temperature. Their results indicated that SiH was dominant at temperatures of around 400 °C, but as the substrate temperature decreased from 275 °C to 50 °C, the number of SiH decreased, while both SiH₂ and SiH₃ appeared, and progressively increased in number. Their results also indicated that SiH₂ and SiH₃ were easily decomposed to SiH, and that the rate of SiH decomposition was much lower than that of SiH₂ and SiH₃.

All of the above studies provide useful information about the dissociative chemisorption of disilane on the Si(001) surface. A comprehensive understanding of the decomposition of disilane, and the role played by the various intermediate species in the silicon forming process, however, is still hampered by a lack of detailed knowledge. The aim of this paper is to model theoretically the various chemisorption structures that could arise from the decomposition of disilane on the Si(001) surface, and to compare these predicted structures with the currently available experimental data.

II. METHOD AND PROCEDURE

Both molecular dynamics (MD) and potential energy calculations have been employed to study the Si(001)2×1:Si₂H₆ chemisorption system. These have been carried out using the extended Brenner (XB) potential.^{29–30} The original Brenner potential was developed for C-H systems in order to simulate chemical-vapor deposition of diamond films from a gaseous mixture of hydrocarbon atoms, molecules and radicals.^{31–32} The Brenner potential follows the Tersoff³³ formalism and is a multiparticle interatomic potential of the cluster functional type. It takes into account the chemical environment of each bond when calculating the bond energy. Since its original development, this potential has been extended to include silicon.²⁹ Further improvements have involved fitting the bond order correction terms for C-Si-H systems, and modification of the angular function.³⁰

In order to perform geometry optimization and MD simulations using the XB potential, the Si(001)2×1 surface has been modelled by an eight layer slab and a unit cell containing 36 atoms per layer. Two-dimensional periodic boundary conditions were applied in the surface plane. The total energy of the system was minimized with respect to the atomic coordinates of the top six substrate layers as well as those of the adsorbed hydrogen, silicon or Si_xH_y species.

To further characterize the system, and provide a basis against which to check the predictions of the model potential, *ab initio* cluster calculations using the Gaussian 94 code were also performed.³⁴ Clusters consisting of 9 silicon atoms, and 12 hydrogen atoms to terminate the bonds at the edges of the cluster, were used to model a single silicon dimer. The equilibrium configurations were first optimized at the Hartree-Fock (HF) level by minimizing the total energy with respect to the coordinates of the dimer silicon atoms, the second layer silicon atoms, and any chemisorbed atomic hydrogen, silicon atoms or Si_xH_y molecules that are present. The third and fourth layer silicon atoms, and all of the ter-

minating hydrogen atoms, were kept fixed. The final geometry was then obtained by reoptimising this HF minimum energy geometry with respect to the same moving atoms using the B3LYP DFT option in Gaussian 94. This state-of-the-art hybrid functional method for exchange and correlation incorporates an exact HF exchange energy functional (Becke's three-parameter functional³⁵), and a semiempirical combination of a local (Vosko-Wilk-Nusair parameterization³⁶) and nonlocal (Lee-Yang-Parr parameterization^{37–39}) spin density electron correlation functional. All of the geometry optimization calculations were performed using the moderately sophisticated double-zeta basis set 6-31G* which includes one set of *d*-polarization functions for the heavy atoms.^{40,41}

The binding energy of each species was obtained by subtracting from the energy of the original chemisorbed slab or cluster, the sum of the energies of the residual slab or cluster, and the desorbed species. This energy is the net amount of energy required to remove the desorbed species from the surface.

III. RESULTS AND DISCUSSION

A. SiH₃ configurations

To investigate the initial stages of the dissociative chemisorption of disilane, simulations of the interaction of Si₂H₆ molecules with the Si(001)2×1 clean surface were performed using the XB potential. In these simulations the incident energies of the Si₂H₆ molecules were varied from 0.1 to 3.6 eV. Simulations were performed for a range of substrate temperatures from 100 to 700 K. Before the commencement of each simulation the system was brought to thermal equilibrium by integrating for 4000 time steps, with the velocities of all of the slab atoms being rescaled after every 100 time steps. A single Si₂H₆ molecule was then placed at a random position above the surface plane with a given translational energy and randomly assigned aiming point, and the simulation continued until the incident molecule had either become chemisorbed, or had rebounded from the surface. At this point, a second molecule was introduced above the surface with a new randomly assigned position and trajectory. This process was continued until the required number of time steps (usually 100 000–200 000) was completed. During this period typically 4–10 molecules were found to chemisorb per surface unit cell. Each molecule was deemed to be chemisorbed if the distance between its center of mass and the surface plane exhibited four successive minima. During each simulation the atoms in the two bottom layers of the slab were kept fixed in their ideal bulk positions. The next two layers were used as a thermal buffer layer to enable dissipation of the translational energy of the incident molecule(s) into the bulk. Velocity rescaling was not applied to the remainder of the slab, or to the adsorbate molecules, once the initial thermalisation was complete and the simulation proper had commenced.

Four different snapshots of one of these simulations are shown in Fig. 1. In this particular simulation, the incident disilane molecule was initially placed 6 Å above the surface as shown in Fig. 1(a), and directed towards the surface with an initial kinetic energy of 0.1 eV. The substrate temperature was maintained at 300 K. Figure 1(b) shows the Si₂H₆ mol-

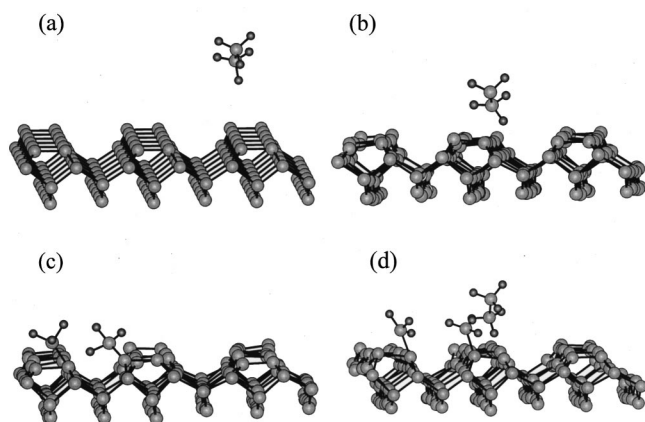


FIG. 1. Sequence of snapshots from a MD simulation of Si_2H_6 molecules interacting with the $\text{Si}(001)2\times 1$ clean surface.

ecule closer to the surface but still intact, while Fig. 1(c) shows the Si_2H_6 molecule dissociated into two SiH_3 radicals, which have become bonded at dangling bond sites. Following this, another Si_2H_6 molecule was introduced into the simulation as illustrated in Fig. 1(d).

During the course of the above simulations only Si_2H_6 dissociation into SiH_3 fragments was observed. This is in agreement with the STM work of Wang *et al.*²⁵ No evidence for the occurrence of either SiH_4 or SiH_2 was seen in these simulations of the initial dissociation of the disilane. Our calculations thus strongly support the dissociation of Si_2H_6 into SiH_3 , but provide no support for the proposed model in which disilane dissociates into SiH_4 and SiH_2 .

Five possible surface configurations for the two SiH_3 radicals produced by the dissociation of a disilane molecule, were observed in our simulations. These are shown in Fig. 2 and correspond to: (1) chemisorption on a single dimer, (2) chemisorption onto adjacent dimers in the same dimer row, (3) adsorption on adjacent dimers in neighboring dimer rows, (4) adsorption on dimers in neighboring rows but separated by one lattice spacing, and (5) adsorption on opposite ends of two adjacent dimers in the same row. Suda *et al.*¹⁹ suggested

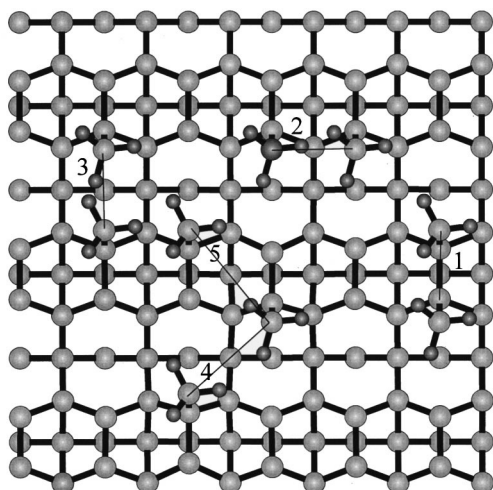


FIG. 2. Top view schematic of a $\text{Si}(001)2\times 1$ surface showing five possible configurations formed from the chemisorption of two SiH_3 radicals at adjacent surface sites.

four possible configurations of the SiH_3 fragments arising from the dissociation of a Si_2H_6 molecule on the $\text{Si}(001)2\times 1$ surface. All four of these surface structures were reproduced by our simulations. They correspond to configurations 1 to 4 in Fig. 2. Suda *et al.* predicted configuration (3) to be unlikely on the grounds that the spacing between the two SiH_3 molecules would be too small. On the basis of simple topographical arguments, Lubben *et al.*⁶ have suggested that configurations 1 and 2 are the most likely SiH_3 configurations to occur. Configuration 5, in which the SiH_3 radicals adsorb on opposite ends of two adjacent dimers, has not been proposed in the literature, to our knowledge.

In all five of the above structures, the SiH_3 fragments are seen to chemisorb onto the surface dimer dangling bonds. In fact, this was the only SiH_3 chemisorption mechanism that was observed in our simulations. This is presumably due to the fact that the singly occupied dangling bonds at the ends of each dimer on the $\text{Si}(001)2\times 1$ surface provide easily accessible bonding sites for any SiH_3 molecule incident on the surface. This is also in agreement with experiment. As stated earlier, high-resolution STM images show that the SiH_3 radicals formed from the dissociation of disilane, bond directly to the terminal “dangling bonds” of the Si-Si dimers.²⁵ The same conclusion has been drawn from a variety of other experimental studies.^{19,23}

Geometry optimization calculations using the XB potential show that the binding energy for a single SiH_3 radical adsorbed on one of the dangling bonds of our 36 atom surface unit cell (which corresponds to $1/36$ ML coverage), is 2.99 eV. When a second SiH_3 radical is chemisorbed at the other end of the same dimer, the binding energy per adsorbate molecule is again 2.99 eV. Cluster calculations performed with the XB potential give a binding energy of 2.91 eV for chemisorption of a single SiH_3 , and 2.90 eV per molecule for chemisorption of two SiH_3 radicals at the same surface dimer (see Table I). The binding energy values obtained from *ab initio* HF/DFT cluster calculations are also 2.91 and 2.90 eV, respectively. The geometries for these two bonding configurations obtained from the XB and HF/DFT calculations are shown in Figs. 3 and 4. Good agreement between the geometries predicted by the two methods is observed. For 1 ML coverage, where radicals are chemisorbed at every dangling bond, the average binding energy per molecule predicted by the XB calculations is 2.95 eV (see Table I). This shows that increasing coverage does not produce any significant change in the SiH_3 binding energy.

Potential energy calculations have been performed at $1/18$ ML coverage for each of the five SiH_3 surface configurations that were observed in the MD simulations. These were carried out using the XB potential, and applying periodic boundary conditions to the eight-layer slab. The total energies of the resulting optimised geometries, and details of the corresponding bond lengths and bond angles, are given in Table II. Configuration 5 has been determined to be the lowest energy structure from our XB potential calculations with configurations 1 and 4 being only 0.04 eV higher in energy. Configurations 2 and 3, in which the two SiH_3 radicals are closer together, are predicted to be less stable than configurations 1, 4, and 5. These results are consistent with the prediction of Suda *et al.*¹⁹ that configuration 3 would be unlikely to occur. They provide no support, however, for the

TABLE I. Binding energies (in eV per adsorbed molecule) for the different Si_xH_y configurations on the $\text{Si}(001)2 \times 1$ surface, obtained from the XB surface calculations. Some XB and HF/DFT cluster values are also given for comparison.

Molecule	Coverage	Surface			Cluster			
		Structures	XB	Fig.	XB	Fig.	HF/DFT	Fig.
SiH_3	1 ML		2.95		2.91	3(a)	2.91	3(b)
	1/18 ML	Configuration 1	2.99	2	2.90	4(a)	2.90	4(b)
		Configuration 2	2.90	2				
		Configuration 3	2.91	2				
		Configuration 4	2.99	2				
Configuration 5		3.03	2					
SiH_2	1/36 ML		2.99	2				
	1 ML	on-dimer	3.68		3.61	6(a)	3.42	6(b)
	1/36 ML	on-end	2.09	5				
	1/18 ML	interrow	2.51	5				
		in-dimer	2.43	5				
on-dimer		3.75	5					
intrarow		3.74	5					
Si_2H_2	1/18 ML	on-dimer A	4.83	8				
		on-dimer B	8.07	8				
		on-dimer C	6.21	8				
		intrarow	4.45	8				
		interrow A	4.57	8				
		interrow B	6.53	8				
		interrow C	4.45	8				

suggestion of Lubben *et al.*⁶ that configurations 1 and 2 would be the preferred structures.

B. SiH_2 configurations

As discussed above, it is now well established that the disilane molecules initially dissociate into SiH_3 radicals, which chemisorb onto the dangling bonds of the $\text{Si}(001)2 \times 1$ surface. These chemisorbed SiH_3 molecules are then believed to dissociate into SiH_2 plus a hydrogen atom via the reaction

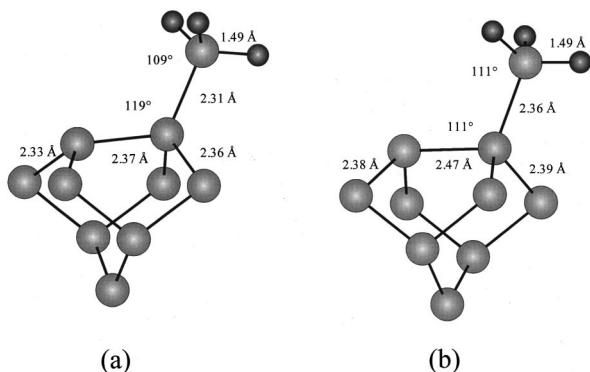


FIG. 3. Optimized cluster geometries corresponding to SiH_3 chemisorption at a dangling bond of the $\text{Si}(001)2 \times 1$ surface; (a) XB and (b) HF/DFT 6-31G*.

This raises two possibilities, either one of the hydrogen atoms is abstracted from the SiH_3 leaving an SiH_2 radical chemisorbed at the dangling bond site, or a ‘‘free’’ SiH_2 radical is created, which subsequently chemisorbs. To investigate the possible SiH_2 structures that can form on the $\text{Si}(001)2 \times 1$ surface we have performed MD simulations based on both of these possibilities.

In the first set of simulations, the initial geometry was taken to be that of a single SiH_2 radical chemisorbed at a dangling bond site of the $\text{Si}(001)2 \times 1$ surface. This geometry, which we shall refer to as the on-end structure, is shown in Fig. 5. In each of these simulations, the system was maintained at constant temperature and simply allowed to evolve in time. During the course of these simulations four different

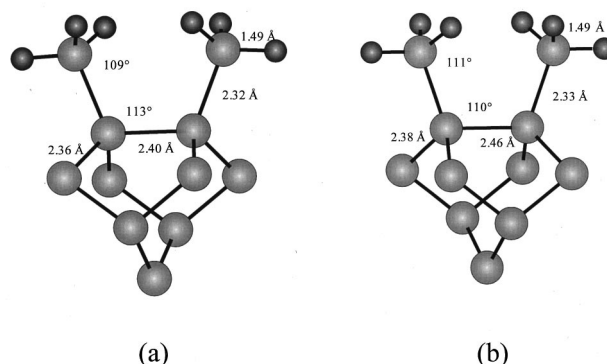


FIG. 4. Optimized cluster geometries for two SiH_3 radicals chemisorbing on the dangling bonds of the same dimer; (a) XB and (b) HF/DFT 6-31 G*.

TABLE II. Total energies (relative to that of configuration 5) and optimized structural parameters for the five different configurations involving two SiH_3 molecules. In this table, and all subsequent tables, a subscript ‘‘a’’ denotes a silicon adsorbate, and a subscript ‘‘d’’ denotes a dimer atom.

Structure	Energy (eV)	Interatomic distances (Å)			Bond angles	
		H-Si _a	Si _a -Si _a	Si _a -Si _d	H-Si _a -H	Si _a -Si _d -Si _d
Configuration 1	0.04	1.49	4.18	2.32	110	113
Configuration 2	0.13	1.49	3.75	2.31	110	119
Configuration 3	0.12	1.49	3.28	2.31	110	119
Configuration 4	0.04	1.49	5.03	2.31	110	119
Configuration 5	0.00	1.49	5.80	2.31	110	120

geometries were observed to occur. These are also shown in Fig. 5 and correspond to: (1) the SiH_2 molecule chemisorbed on top of a dimer at the bridge site with the silicon dimer remaining intact (on-dimer), (2) the SiH_2 molecule chemisorbed on top of a dimer with the silicon dimer bond broken (in-dimer), (3) the SiH_2 molecule chemisorbed at the valley site between two adjacent dimer rows (interrow), and (4) the SiH_2 molecule chemisorbed at the cross-dimer site between two adjacent dimers of the same row (intra-row). All of these structures were suggested by Bronikowski *et al.*²⁴ and have been studied theoretically by Bowler and Goringe²⁶ using the LDA density-functional method.

To determine the relative probability of occurrence of these four SiH_2 configurations, we performed approximately 120 simulations for each of the three temperatures 850, 900, and 1000 K. The results are presented in Table III. We ob-

serve that in 27% of the cases at 850 K, the SiH_2 radical rotated to form the on-dimer structure, whilst in 46% of the cases it has bonded across to a neighboring dimer to form the intrarow structure. The in-dimer and interrow structures occur with considerably smaller probabilities (2% and 4%, respectively). The probability of occurrence of the on-dimer and intrarow structures is seen to decrease significantly with increasing temperature, while that of the in-dimer and interrow configurations increases correspondingly.

In addition to the above calculations, we have also performed MD simulations in which unbonded SiH_2 radicals were allowed to interact with the $\text{Si}(001)2\times 1$ surface. These simulations, which were analogous to those reported earlier for SiH_3 , gave rise to exactly the same SiH_2 configurations as found in the simulations starting from the on-end configuration (i.e., the on-dimer, in-dimer, interrow and intrarow, structures). Some of the SiH_2 radicals were also observed to chemisorb onto a dangling bond at the end of a dimer to form the on-end structure.

The minimum energy topologies of these SiH_2 configurations were determined by performing potential energy calculations at $T=0$ K using the extended Brenner potential. The energies of all of the configurations (including the on-end structure), and values for the corresponding bond lengths and bond angles, are given in Table IV. Also presented in this table are the LDA results obtained by Bowler and Goringe²⁶ for the on-dimer, in-dimer, interrow and intrarow structures. Good agreement between the bondlengths and bond angles predicted by the XB and LDA calculations is apparent for these four structures. The SiH_2 binding energies predicted by the XB potential calculations for all of the SiH_2 structures are given in Table I.

Of all of the $\text{Si}(001):\text{SiH}_2$ configurations at 1/18 ML coverage which we have examined, the overall minimum energy structure predicted by the XB potential, is the on-dimer structure. The XB binding energy values of 3.68 eV (1 ML),

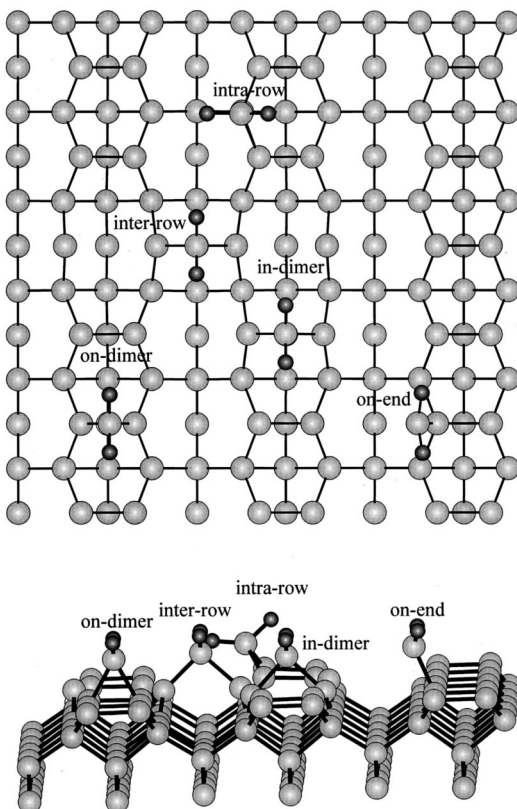


FIG. 5. Top and side views of the $\text{Si}(001)2\times 1$ surface showing the five SiH_2 configurations which have been investigated in this study.

TABLE III. The probability of occurrence of the various SiH_2 configurations at the temperatures 850, 900, and 1000 K.

Structure/T(K)	850	900	1000
on-dimer	27%	24%	21%
intrarow	46%	35%	29%
interrow	4%	12%	14%
in-dimer	2%	7%	10%
unbonded	21%	22%	26%

TABLE IV. Total energies (relative to the on-dimer configuration), interatomic distances and bond angles for the different SiH₂ configurations. The data in the brackets has been obtained from *ab initio* DFT slab calculations (Ref. 26).

Configuration	Energy (eV)	Interatomic distance (Å)			Bond angles (°)	
		H-Si _a	Si _a -Si _d	Si _d -Si _d	H-Si _a -Si _d	Si _d -Si _a -Si _d
on-end	1.66	1.51	2.28	2.37	115	30
in-dimer	1.32 (0.18)	1.48	2.34 (2.31)	3.26 (3.29)	114 (113)	88 (91)
interrow	1.24 (0.31)	1.49	2.35 (2.37)	3.93 (3.92)	113 (109)	93 (105)
intrarow	0.014 (-0.004)	1.48	2.39 (2.41)	2.35 (2.40)	113 (121)	92 (92)
on-dimer	0.00 (0.00)	1.48	2.42 (2.32)	2.44 (2.43)	118 (118)	61 (63)

3.75 eV (1/18 ML), and 3.61 eV (cluster), are all in very good agreement with our HF/DFT calculated result of 3.42 eV (see Table I). The on-dimer topologies obtained from the XB and HF/DFT cluster calculations are shown in Fig. 6 and are seen to be in excellent agreement. The LDA calculations of Bowler and Goringe²⁶ predict the intrarow structure to be the minimum energy configuration and more stable than the on-dimer structure by 0.004 eV. The binding energy of this structure is predicted by our 1/18 ML XB calculations to be 3.74 eV, just 0.01 eV less than for the on-dimer structure.

The STM images of Bronikowski *et al.*²⁴ indicate that each SiH₂ radical occupies a bridging position between two adjacent dimers of the same dimer row, but provide no evidence for an SiH₂ occupying the bridging position directly above a single dimer. The experimental data would thus appear to provide strong support for the intrarow model, but not for the on-dimer topology. While the formation of the on-dimer structure would appear to be unlikely due to large bond angle distortions, both the LDA and XB calculations predict that the on-dimer and intrarow structures are nearly degenerate in energy. Our MD simulations also suggest that the on-dimer structure should occur. The higher probability of occurrence of the intrarow structure in the MD simulations does, however, indicate a lower activation barrier for the formation of this structure than for the on-dimer structure. This may explain why the intrarow structure has been observed in the STM topographs, but not the on-dimer structure.

The MD simulations showed that the in-dimer structure was relatively unstable and would readily change into the on-dimer configuration. This is consistent with the calculated binding energy of 2.43 eV obtained from the XB potential

for the in-dimer structure. This is 1.32 eV smaller than the calculated binding energy for the on-dimer structure due to the dimer σ bond being broken. These results are in qualitative agreement with the LDA calculations,²⁶ which also predict that the in-dimer structure is less energetically favorable than the on-dimer structure. HF/DFT geometry optimization calculations for the in-dimer structure failed to yield a local minimum. Even starting the optimization procedure from this structure always resulted in the on-dimer topology as the ground-state configuration.

To form the interrow structure both of the surface dimers which are bonded to the adsorbed SiH₂ molecule have to break (see Fig. 5). This results in this structure being relatively unfavorable energetically: Its XB calculated binding energy is only 2.51 eV. This is very close to that of the in-dimer structure (2.43 eV), and 1.24 eV smaller than the minimum energy on-dimer structure. This relative instability of the interrow structure is consistent with both the LDA calculations,²⁶ and the low probability of occurrence of this structure in our MD simulations.

C. Si₂H₂ configurations

Two different models have been proposed in the literature for the growth of epitaxial silicon on the Si(001)2×1 surface from the SiH₂ radicals that result from the dissociation of disilane.^{19,21,25} In the first of these models, SiH₂ radicals are chemisorbed at the bridge sites of two adjacent dimers of the same row with the H-Si-H direction of each radical lying along the dimer row. The two neighboring hydrogen atoms bond together to form H₂, which desorbs from the surface, leaving an H-Si-Si-H (Si₂H₂) configuration centred on the pedestal site between the two dimers. Further hydrogen desorption from this H-Si-Si-H structure results in a Si-Si dimer oriented perpendicular to the underlying dimers as observed in the normal silicon epitaxial growth process. This model has been proposed by both Suda *et al.*¹⁹ and Boland,²¹ and is shown schematically in Fig. 7(a)

In the second model, each SiH₂ radical bridges across the ends of two adjacent dimers of a given dimer row with one SiH₂ being linked with one dimer row and the other SiH₂ with the neighboring dimer row, so that these two radicals are immediately adjacent to one another. The two neighboring H are again assumed to combine to form H₂, which desorbs from the surface, leaving a H-Si-Si-H combination. Desorption of the remaining hydrogen produces a Si-Si dimer parallel to the underlying dimers. This is the model proposed by Wang *et al.*²⁵ and is shown schematically in

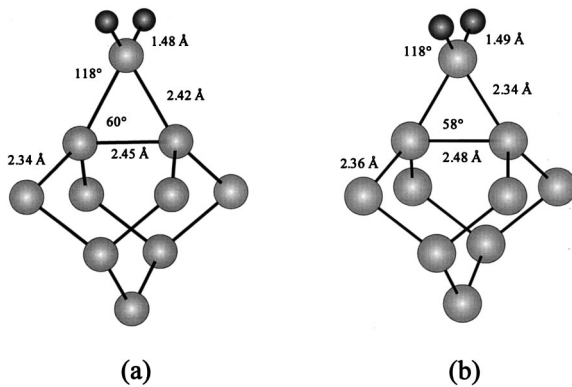


FIG. 6. Optimized cluster geometries for the SiH₂ on-dimer structure; (a) XB and (b) HF/DFT 6-31G*.

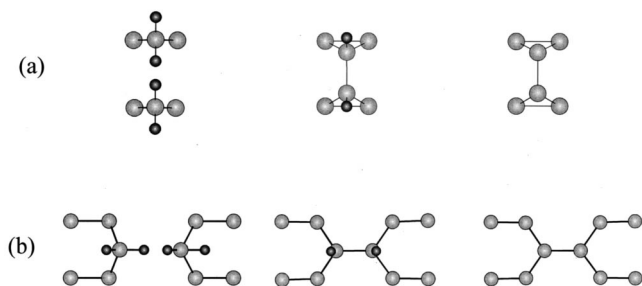


FIG. 7. Proposed mechanisms for the interaction of SiH_2 radicals on the $\text{Si}(001)2 \times 1$ surface, and the formation of H-Si-Si-H complexes, as a precursor to the establishment of Si-Si ad-dimers; (a) proposed in Refs. 19 and 21, (b) proposed in Ref. 25.

Fig. 7(b). Strong support for this model comes from the STM work, which has been interpreted as showing both SiH_2 radicals bridge bonded across the ends of two neighboring dimers of the same row, and the corresponding H-Si-Si-H complexes.²⁵ A possible problem with this model, however, is the predicted orientation of the resulting ad-dimers being different from that observed in normal silicon epitaxial growth, and the energy that would be required to re-align them. Such Si-Si ad-dimers have been observed in the STM images,²⁵ but they are not as common as those oriented along the normal epitaxial growth direction; that is, perpendicular to the substrate dimers.

To investigate these two possible models we have performed a number of different calculations. In the first set of calculations, we set up the initial Si_2H_4 structures assumed in these models within our large surface unit cell by placing two adjacent SiH_2 radicals in the on-dimer and intrarow configurations, respectively. We then optimized the geometry with our MD code using periodic boundary conditions. The two structures were found to yield very similar energies with the on-dimer-based structure being slightly more stable by 0.06 eV.

We then considered a number of H-Si-Si-H (Si_2H_2) configurations that might form on the $\text{Si}(001)2 \times 1$ surface. Figure 8 presents top and side views of these different possible bonding configurations. Local minima in the potential energy surface were found to exist for each of these chemisorption configurations. These configurations correspond to: (1) the Si_2H_2 complex centered on the bridge site of a single dimer (on-dimer A), (2) the Si_2H_2 complex positioned above the pedestal site of two neighboring dimers with the Si-Si bond oriented along the dimer row (on-dimer B), (3) the Si_2H_2 complex sited at the pedestal site between two adjacent dimers with the Si-Si bond oriented parallel to the dimer bonds (on-dimer C), (4) the Si_2H_2 complex chemisorbed above the bridging site across the ends of two adjacent dimers from the same row (intra-row), (5) the Si_2H_2 complex positioned above the valley site and connected to two dimers from different rows (interrow A), (6) the Si_2H_2 complex centered on the cave site between two dimer rows, bonded to four Si dimer atoms, and oriented parallel to the dimer bonds (interrow B), and (7) the Si_2H_2 complex positioned above the cave site, connected to four Si dimer atoms, and oriented parallel to the dimer rows (interrow C). The calculated binding energies for these seven possible structures are given in

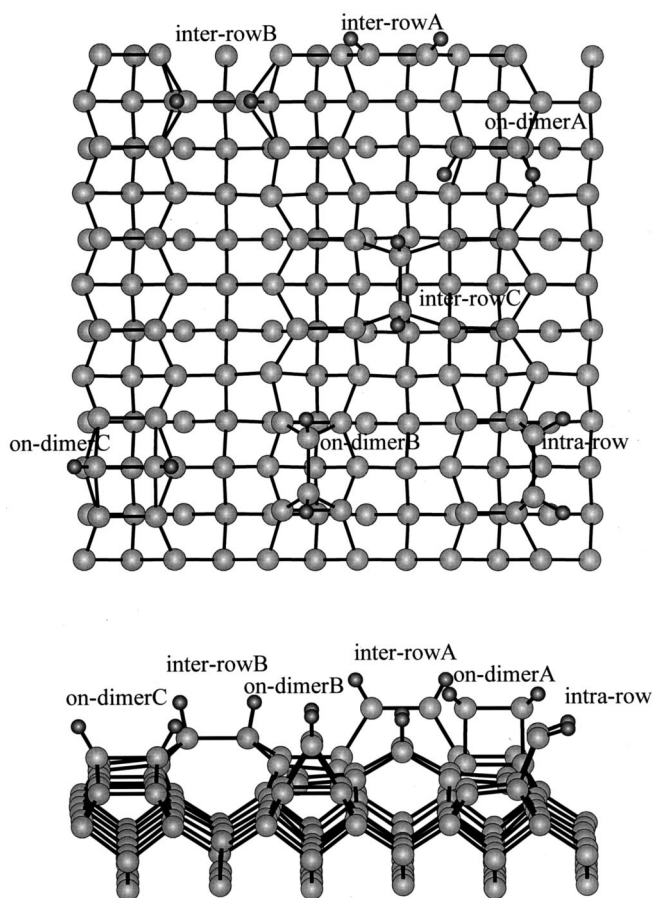


FIG. 8. Top and side views of the $\text{Si}(001)2 \times 1$ surface showing the seven possible H-Si-Si-H configurations, which have been investigated in this study.

Table I. Values for the relative total energies and characteristic bondlengths and bond angles are given in Table V.

The most stable structure of these seven possible configurations is predicted to be the on-dimer B structure (configuration 2) in which the Si_2H_2 complex is centered on the pedestal site between two adjacent dimers with the Si-Si bond of the molecule oriented along the dimer row. This structure is identical to that proposed by Suda *et al.*¹⁹ and Boland,²¹ and has a Si_2H_2 binding energy of 8.07 eV. The various structural parameters which characterize this configuration are listed in Table V. We observe that the two silicon dimers, which are bonded to the adsorbed Si_2H_2 complex have stretched from 2.30 to 2.45 Å and moved closer together (see Table V and Fig. 8).

The second most stable structure is the interrow B structure (configuration 6) in which the H-Si-Si-H complex is positioned above a cave site equidistant from all four dimers (see Fig. 8). This is the model proposed by Wang *et al.*²⁵ on the basis of their STM images of disilane chemisorption on the $\text{Si}(001)2 \times 1$ surface. Our XB potential calculations predict that this configuration has a Si_2H_2 binding energy of 6.53 eV, and hence is 1.54 eV less stable than the on-dimer B structure. The geometrical parameters characterising this structure are also given in Table V. We observe that all four silicon dimers that are bonded to the Si_2H_2 complex move inward and have their dimer bondlengths stretched from 2.30 to 2.36 Å.

TABLE V. Total energies (relative on the on-dimer *B* structure), interatomic distances, and bond angles for the different Si₂H₂ configurations.

Configuration	Energy (eV)	Interatomic distance (Å)				Bond angles		
		H-Si _a	Si _a -Si _a	Si _d -Si _d	Si _a -Si _d	Si _d -Si _a -Si _a	H-Si _a -Si _d	H-Si _a -Si _a
intrarow	3.62	1.48	2.35	2.38	2.38	106	117	117
interrow <i>C</i>	3.62	1.50	2.36	2.42	2.38	106	110	112
interrow <i>A</i>	3.51	1.48	2.35	2.39	2.37	120	117	117
on-dimer <i>A</i>	3.24	1.48	2.36	2.41	2.38	91	117	117
on-dimer <i>C</i>	1.86	1.52	2.51	2.37	2.46	88	120	120
interrow <i>B</i>	1.54	1.54	2.42	2.36	2.48	121	108	101
on-dimer <i>B</i>	0.00	1.50	2.32	2.45	2.41	106	124	121

The only other structure based on our calculations, which might be likely to occur in practice is the on-dimer *C* configuration (configuration 3). This configuration differs from the on-dimer *B* structure in that the Si₂H₂ complex is rotated by 90° so that the Si-Si bond is oriented perpendicular to the dimer rows (see Fig. 8). The two silicon dimers connected to the Si₂H₂ molecule are again expanded with their bondlengths being 2.37 Å, 0.07 Å more than that for the clean surface. The binding energy of the Si₂H₂ in this configuration is predicted to be 6.21 eV, just 0.32 eV less than that of the interrow *B* structure.

IV. DISCUSSION AND CONCLUSIONS

In this paper, we have performed molecular-dynamics simulations and potential energy calculations with the extended Brenner potential to investigate the dissociative chemisorption of disilane on the Si(001)2×1 surface. MD simulations in which Si₂H₆ molecules were allowed to impinge on the Si(001)2×1 surface with a variety of different incident energies, and at various temperatures, have shown that the disilane molecules dissociate into SiH₃ fragments which then chemisorb onto the surface dimer dangling bonds. This is consistent with recent experimental work. Five different chemisorption configurations have been found, which involve pairs of SiH₃ radicals. The most energetically stable of these configurations is found to be that in which the SiH₃ molecules chemisorb on opposite ends of two adjacent dimers from the same row.

Molecular-dynamics simulations have also been employed to study the behavior of a SiH₂ radical that is bonded to a Si-Si surface dimer in the on-end configuration. Four SiH₂ configurations were observed to occur in these simulations. Exactly the same configurations were obtained from MD simulations of unbonded SiH₂ radicals incident on the surface. Zero temperature geometry optimization calculations for these SiH₂ structures using the XB potential produced results in very good agreement with the LDA calculations of Bowler and Goringe.²⁶ The on-dimer and intrarow

structures were found to be nearly degenerate in energy and to constitute the most energetically favourable SiH₂ chemisorption structures on the Si(001) surface. This result is in agreement with the earlier LDA calculations.²⁶ It is also consistent with the MD simulations, which showed that both the on-dimer and intrarow structures occurred with a fairly high probability, while the other structures were characterized by much smaller probabilities. All of this work would suggest that both the on-dimer and intrarow topologies should occur as part of the normal disilane silicon growth process. To date, however, only the intrarow model has been confirmed experimentally with the STM topographs of Wang *et al.*²⁵ providing strong evidence of SiH₂ complexes bridge bonding across the ends of two adjacent dimers of the same row. To our knowledge, there has been no experimental observation of the on-dimer SiH₂ structure.

Two different models have been proposed for the interaction of SiH₂ complexes on the Si(001)2×1 surface, and the subsequent formation of a H-Si-Si-H complex. Both of these proposed structures have been investigated in this paper, together with five other possible Si₂H₂ structures. The most energetically favorable structure was found to be the on-dimer *B* structure. This is the structure proposed by Suda *et al.*¹⁹ and Boland,²¹ and is based on the assumption that the SiH₂ are bonded at the dimer bridge sites. While this H-Si-Si-H structure does not appear to have been observed experimentally, it does predict the correct orientation of the resultant ad-dimers. The second most energetically favourable structure predicted by the XB calculations was the intra-row structure proposed by Wang *et al.*²⁵ This structure is consistent with the observed bridge-bonding of SiH₂ between the ends of two adjacent dimers, and has been observed in the STM topographs of Wang *et al.*,²⁵ but requires rotation of the resultant ad-dimers to yield the normal epitaxial growth pattern.

ACKNOWLEDGMENT

J-Z. Que would like to acknowledge the University of Newcastle for financial support.

*Author to whom correspondence should be addressed. FAX: 61-2-49216907. Electronic address: adam@linus.newcastle.edu.au

¹F. Mieno, S. Nakamura, T. Deguchi, M. Maeda, and K. Inayoshi, *J. Electrochem. Soc.* **134**, 2320 (1987).

²H. Hirayama, T. Tatsumi, and N. Aiziki, *Appl. Phys. Lett.* **52**, 1484 (1988).

³D-S. Lin, E. S. Hirschorn, T-C. Chiang, R. Tsu, D. Lubben, and J. E. Greene, *Phys. Rev. B* **45**, 3494 (1992).

- ⁴A. Yoshikawa and S. Yamaga, *Jpn. J. Appl. Phys., Part 2* **23**, L91 (1984).
- ⁵Y. Suda, D. Lubben, T. Motooka, and J. E. Greene, *J. Vac. Sci. Technol. B* **7**, 1171 (1989).
- ⁶D. Lubben, R. Tsu, T. R. Bramblett, and J. E. Greene, *J. Vac. Sci. Technol. A* **9**, 3003 (1991).
- ⁷R. Tsu, D. Lubben, T. R. Bramblett, J. E. Greene, D-S. Lin, and T-C. Chiang, *Surf. Sci.* **280**, 265 (1993).
- ⁸R. Tsu, H. Z. Xiao, Y-W. Kim, M. A. Hasan, H. K. Birnbaum, J. E. Greene, D-S. Lin, and T-C. Chiang, *J. Appl. Phys.* **75**, 240 (1994).
- ⁹T. R. Bramblett, Q. Lu, T. Karasawa, M. A. Hasan, S. K. Jo, and J. E. Greene, *J. Appl. Phys.* **76**, 1884 (1994).
- ¹⁰S. M. Mokler, *Crit. Rev. Surf. Chem.* **4**, 1 (1994).
- ¹¹S. M. Gates, *Surf. Sci.* **195**, 307 (1988).
- ¹²S. M. Gates, C. M. Greenlief, D. B. Beach, and P. A. Holbert, *J. Chem. Phys.* **92**, 3144 (1990).
- ¹³K. F. Roenigk, K. F. Jensen, and R. W. Carr, *J. Phys. Chem.* **91**, 5732 (1987).
- ¹⁴J. G. Martin, M. A. Ring, and H. E. O'Neal, *Int. J. Chem. Kinet.* **19**, 715 (1987).
- ¹⁵S. M. Gates and C. M. Chiang, *Chem. Phys. Lett.* **184**, 448 (1991).
- ¹⁶S. M. Gates and S. K. Kulkarni, *Appl. Phys. Lett.* **60**, 53 (1992).
- ¹⁷P. Jakob, Y. J. Chabal, and K. Raghavachari, *Chem. Phys. Lett.* **187**, 325 (1991).
- ¹⁸K. W. Kolasinsky, S. F. Shane, and R. N. Zare, *J. Chem. Phys.* **96**, 3995 (1992).
- ¹⁹Y. Suda, D. Lubben, T. Motooka, and J. E. Greene, *J. Vac. Sci. Technol. A* **8**, 61 (1990).
- ²⁰R. Imbihl, J. E. Demuth, S. M. Gates, and B. A. Scott, *Phys. Rev. B* **39**, 5222 (1989).
- ²¹J. J. Boland, *Phys. Rev. B* **44**, 1383 (1991).
- ²²D-S. Lin, T. Miller, T-C. Chiang, R. Tsu, and J. E. Greene, *Phys. Rev. B* **48**, 11 846 (1993).
- ²³S. M. Gates, C. M. Greenlief, and D. B. Beach, *J. Chem. Phys.* **93**, 7493 (1990).
- ²⁴M. J. Bronikowski, Y. Wang, M. T. McEllistrem, D. Chen, and R. J. Hamers, *Surf. Sci.* **298**, 50 (1993).
- ²⁵Y. Wang, M. J. Bronikowski, and R. J. Hamers, *Surf. Sci.* **311**, 64 (1994).
- ²⁶D. R. Bowler and C. M. Goringe, *Surf. Sci.* **360**, L489 (1996).
- ²⁷J. H. G. Owen, D. R. Bowler, C. M. Goringe, K. Miki, and G. A. D. Briggs, *Surf. Sci.* **382**, L678 (1997).
- ²⁸A. Yoshigoe, K. Mase, Y. Tsusaka, and T. Urisu, *Appl. Phys. Lett.* **67**, 2364 (1995).
- ²⁹A. J. Dyson and P. V. Smith, *Surf. Sci.* **355**, 140 (1996).
- ³⁰A. J. Dyson and P. V. Smith, *Mol. Phys.* **96**, 1491 (1999).
- ³¹D. W. Brenner, *Phys. Rev. B* **42**, 9458 (1990).
- ³²D. W. Brenner, J. A. Harrison, C. T. White, and R. J. Colton, *Thin Solid Films* **206**, 220 (1991).
- ³³J. Tersoff, *Phys. Rev. Lett.* **56**, 632 (1986).
- ³⁴M. J. Frisch, G. W. Trucks, H. B. Schlegel, P. W. M. Gill, B. G. Johnson, M. A. Robb, J. R. Cheeseman, T. A. Keith, G. A. Petersson, J. A. Montgomery, K. Raghavachari, M. A. Al-Laham, V. G. Zakrzewski, J. V. Ortiz, J. B. Foresman, J. Cioslowski, B. B. Stefanov, A. Nanayakkara, M. Challacombe, C. Y. Peng, P. Y. Ayala, W. Chen, M. W. Wong, J. L. Andres, E. S. Replogle, R. Gomperts, R. L. Martin, D. J. Fox, J. S. Binkley, D. J. Defrees, J. Baker, J. P. Stewart, M. Head-Gordon, C. Gonzalez, and J. A. Pople, *Gaussian 94*, Revision D.4 (Gaussian Inc., Pittsburgh, PA, 1995).
- ³⁵A. D. Becke, *J. Chem. Phys.* **98**, 5648 (1993).
- ³⁶S. H. Vosko, L. Wilk, and M. Nusair, *Can. J. Phys.* **58**, 1200 (1980).
- ³⁷C. Lee, W. Yang, and R. G. Parr, *Phys. Rev. B* **37**, 785 (1988).
- ³⁸A. D. Becke, *Phys. Rev. A* **38**, 3098 (1988).
- ³⁹B. Miehlich, A. Savin, H. Stoll, and H. Preuss, *Chem. Phys. Lett.* **157**, 200 (1989).
- ⁴⁰G. A. Petersson and M. A. Al-Laham, *J. Chem. Phys.* **94**, 6081 (1991).
- ⁴¹G. A. Petersson, A. Bennett, T. G. Tensfeldt, M. A. Al-Laham, W. A. Shirley, and J. Mantzaris, *J. Chem. Phys.* **89**, 2193 (1988).